Synthesis and Computational Studies of Palladium(I) Dimers $Pd_2X_2(P^tBu_2Ph)_2$ (X = Br, I): Phenyl versus Halide Bridging Modes

Ute Christmann,[§,†] Dimitrios A. Pantazis,[‡] Jordi Benet-Buchholz,[†] John E. McGrady,*[,‡] Feliu Maseras,[†,⊥] and Ramón Vilar*[,§,†]

Department of Chemistry, Imperial College London, South Kensington, London SW7 2AZ, U.K., Institute of Chemical Research of Catalonia (ICIQ), Avgda. Països Catalans 16, 43007, Tarragona, Spain, WestCHEM, Department of Chemistry, Joseph Black Building, University of Glasgow, G12 8QQ, U.K., and Unitat de Química Física, Edifici Cn, Universitat Autònoma de Barcelona, 08193 Bellaterra, Catalonia, Spain

Received August 7, 2006

The synthesis and characterization of the new palladium(I) dimer $Pd_2Br_2(\mu\text{-}P^tBu_2Ph)_2$ (**8**) is reported herein. The single-crystal X-ray analysis of this compound has shown that the phosphine acts as a bridging ligand between the two palladium centers, using the phosphorus atom as well as the *ipso*- and *ortho*-carbon atoms of the phenyl substituents. An analysis of the electronic structure indicates that the bond between the remote palladium center and the bridging ligand is stabilized by two distinct electronic components, one with the C=C bond of the arene, the other an agostic-type interaction with the P−C bond. The steric bulk at the phosphorus center causes distinct changes in the relative contributions of these two components and, hence, distorts the structure. In contrast, the iodide analogue (**9**) adopts a completely different structure, where the phosphines are terminally coordinated and the halide acts as a bridging ligand.

Introduction

Dinuclear Pd^I-Pd^I complexes have received considerable attention over the past few years as a result of their ability to react with a wide range of substrates, with important potential applications in organometallic catalysis.[1−6] The reactivity of the dimers (whether the metal−metal bond is bridged or unsupported) is highly dependent on the ligands coordinated to the palladium centers, and so the development of synthetic routes to this type of complex with ligands that have a wide range of electronic and steric properties remains a subject of great interest. Phosphines are particularly suitable in this regard since their size and electronic properties can be readily modulated, they coordinate easily to palladium, and the resulting compounds can be monitored experimentally by means of ^{31}P NMR spectroscopy.

Over the past few years, we have investigated the synthesis, reactivity, and catalytic properties of several palladium dimers containing sterically demanding phosphines.[7−9] More specifically, we have reported the preparation and structural characterization of the dinuclear halide-bridged species $Pd_2(\mu\text{-}X)_2(P^tBu_3)_2$ (X = Br, **1**; I, **2**) shown in Scheme 1. These compounds, which can be prepared by either a comproportionation reaction or oxidative addition of halides to palladium(0) species, have a strained $Pd_2(\mu\text{-}X)_2$ core and show a rich reactivity toward a wide range of small molecules (e.g., CO, CNR, O_2, and C_2R_2). A few years after these compounds were first reported, Hartwig demonstrated that the bromide complex $Pd_2(\mu\text{-}Br)_2(P^tBu_3)_2$ is an excellent precatalyst for the amination of aryl halides.[10] The high reactivity of this system has been attributed to the in situ generation of monophosphine palladium complexes that can readily undergo oxidative-addition of aryl halides.

The unique catalytic properties of these palladium dimers with low phosphine-to-palladium ratio[11] prompted us to explore the synthesis and properties of a new series of palladium dinuclear complexes containing biphenyl phosphines (complexes **3**−**7** in Scheme 1),[9,12] where the biphenyl group adopts an unusual $\eta^2{:}\eta^2$ bridging mode. Besides their unique structural properties, these complexes have also proved to be excellent precatalysts for the amination of aryl chlorides and bromides.

Given the strongly contrasting structural and catalytic properties of the P^tBu_3 and P^tBu_2(Bph-R) dimers, we decided to explore the properties of analogous dinuclear complexes containing P^tBu_2Ph. This phosphine offers the possibility of π-coordination via its phenyl ring, but the metal−phenyl interactions are not expected to be as strong as those in the P^tBu_2(Bph-R) analogues, where the phenyl ring can approach the remote palladium center more closely. Herein we report the

* Corresponding authors. E-mail: r.vilar@imperial.ac.uk; j.mcgrady@chem.gla.ac.uk.
§ Imperial College London.
† ICIQ.
‡ University of Glasgow.
⊥ Universitat Autònoma de Barcelona.

(1) Sui-Seng, C.; Enright, G. D.; Zargarian, D. *J. Am. Chem. Soc.* **2006**, *128*, 6508.
(2) Barder, T. E. *J. Am. Chem. Soc.* **2006**, *128*, 898.
(3) Murahashi, T.; Kurosawa, H. *Coord. Chem. Rev.* **2002**, *231*, 207.
(4) Lin, W.; Wilson, S. R.; Girolami, G. S. *Inorg. Chem.* **1994**, *33*, 2265.
(5) Dupont, J.; Pfeffer, M.; Rotteveel, M. A.; De Cian, A.; Fischer, J. *Organometallics* **1989**, *8*, 1116.
(6) Kannan, S.; James, A. J.; Sharp, P. R. *J. Am. Chem. Soc.* **1998**, *120*, 215.
(7) Dura-Vila, V.; Mingos, D. M. P.; Vilar, R.; White, A. J. P.; Williams, D. J. *J. Organomet. Chem.* **2000**, *600*, 198.
(8) Vilar, R.; Mingos, D. M. P.; Cardin, C. J. *J. Chem. Soc., Dalton Trans.* **1996**, 4313.
(9) Christmann, U.; Vilar, R.; White, A. J. P.; Williams, D. J. *Chem. Commun.* **2004**, 1294.
(10) Stambuli, J. P.; Kuwano, R.; Hartwig, J. F. *Angew. Chem., Int. Ed.* **2002**, *41*, 4746.
(11) Christmann, U.; Vilar, R. *Angew. Chem., Int. Ed.* **2005**, *44*, 366.
(12) Christmann, U.; Pantazis, D. A.; Benet-Buchholz, J.; McGrady, J. E.; Maseras, F.; Vilar, R. *J. Am. Chem. Soc.* **2006**, *128*, 6376.

10.1021/om060712j CCC: $33.50
Publication on Web 11/15/2006

Scheme 1

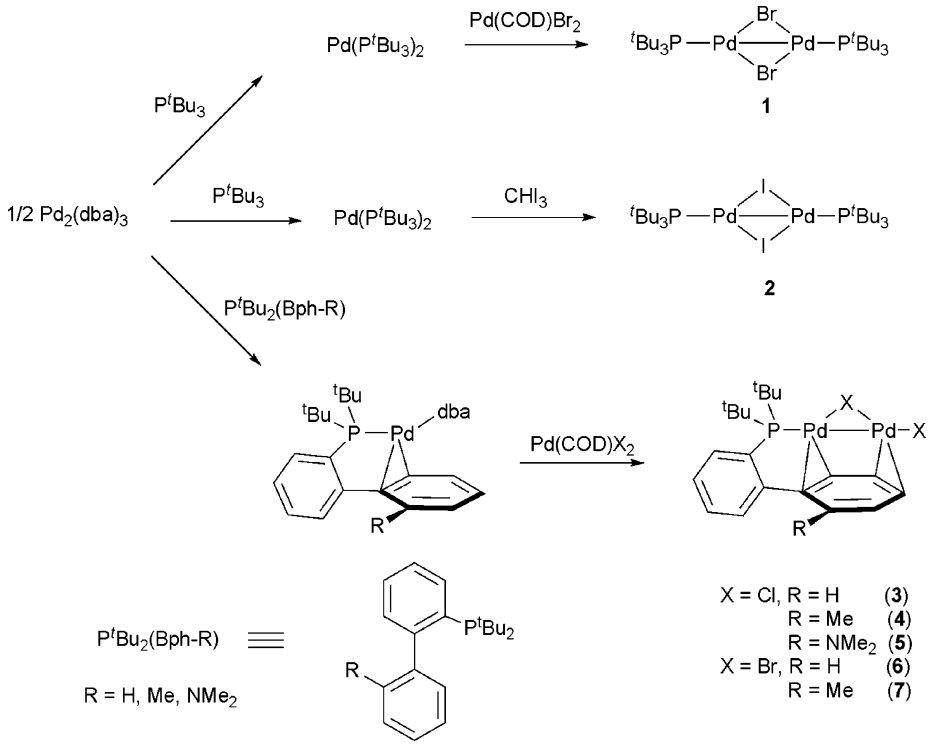

Scheme 2

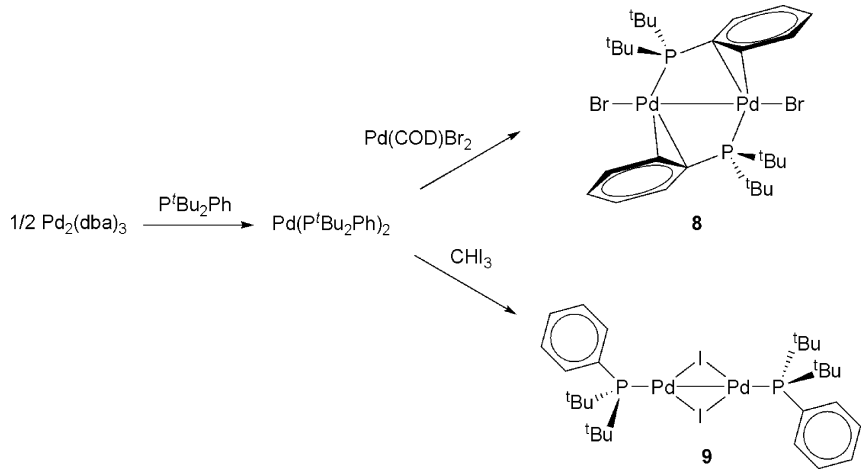

synthesis and characterization of the new palladium(I) dimers $Pd_2Br_2(\mu\text{-}P^tBu_2Ph)_2$ (**8**) and $Pd_2(\mu\text{-}I)_2(P^tBu_2Ph)_2$ (**9**) including the single-crystal X-ray crystallographic analysis of **8**. An analysis of the electronic structure of these dimers has also shed some light on the factors that control the ligand coordination modes.

Results and Discussion

Synthesis and Structural Characterization of $Pd_2Br_2(\mu\text{-}P^tBu_2Ph)_2$ (8). When 1 equiv of $Pd_2(dba)_3$ was mixed with 4 equiv of P^tBu_2Ph and stirred for 2 h, the $^{31}P\{^1H\}$ NMR spectrum of the reaction solution showed a single resonance at 67.7 ppm that corresponds to the chemical shift previously reported for $Pd(P^tBu_2Ph)_2$ (see Scheme 2).[13] Addition of $Pd(COD)Br_2$ to this solution caused an immediate change in color from orange to brown and a dark precipitate formed. After a further 3 h, filtration yielded a brown solid, which was washed with diethyl ether and recrystallized from CH_2Cl_2/hexane.

The $^{31}P\{^1H\}$ NMR spectrum of this solid exhibits a singlet at δ 76.9 ppm, while the FAB(+) mass spectrum shows the expected fragmentation pattern for a compound with the formulation $Pd_2Br_2(P^tBu_2Ph)_2$. The highest intensity peak, which is observed at 737 amu, can be assigned to $[M - Br]^+$, while a smaller peak at 818 amu corresponds to $[M]^+$. Single crystals of this compound (**8**) suitable for X-ray crystallographic analysis were grown from a chloroform solution.

The molecular structure of **8** (Figure 1) confirms that this complex is indeed a palladium(I) dimer, but the coordination geometry is dramatically different from the P^tBu_3 species **1**, where the two bromide ligands occupy bridging positions. In this case each phosphine is directly coordinated to one of the palladium centers via the phosphorus atom but also to the second palladium via the phenyl substituent on the phosphine. Bonds to the *ipso*-carbon atoms of the phenyl rings are relatively short

(13) Mann, B. E.; Musco, A. *J. Chem. Soc., Dalton Trans.* **1975**, 1673.

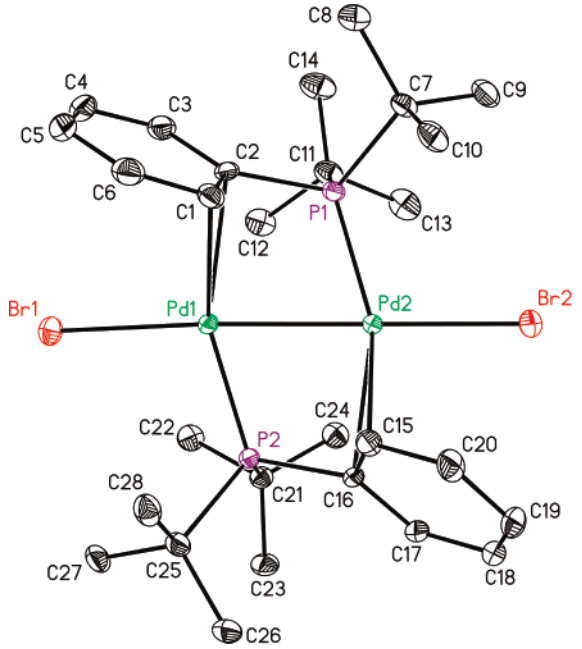

Figure 1. ORTEP plot (thermal ellipsoids shown at 50% probability level) of **8**. Hydrogen atoms have been omitted for the sake of clarity. Selected distances (Å) and angles (deg): Pd1−Pd2, 2.5706(4); Pd1−Br1, 2.5287(5); Pd2−Br2, 2.5018(5); Pd1−C1, 2.469(3), Pd1−C2, 2.403(3); Pd1−P2, 2.2440(8); Pd1−P1, 2.9217-(8); Pd2−C15, 2.448(3); Pd2−C16, 2.421(3); Pd2−P1, 2.2416(8); Pd2−P2, 2.8927(8); P1−C2, 1.834(3); P2−C16, 1.826(2); C1−C2, 1.419(4); C15−C16, 1.411(4); Pd1−Pd2−Br2, 175.316-(13); Pd2−Pd1−Br1, 172.843(11); Pd1−P2−C16, 108.00(9); Pd2−P1−C2, 107.36(9); Pd1−C2−C1, 75.64(16); Pd2−C16−C15, 74.24(16).

(2.403(3) Å [Pd1−C2] and 2.421(3) Å [Pd2−C16]), while those to the *ortho*-carbons are slightly longer (2.469(3) Å [Pd1−C1] and 2.448(3) Å [Pd2−C15]). All four distances are consistent with a significant interaction between the arene ring and the corresponding palladium atom. On the other hand, the Pd(1)···P(1) and Pd(2)···P(2) separations of 2.92 Å suggest only a weak interaction between the palladium centers and the corresponding distal phosphine. The NMR spectroscopic data of **8** in solution are fully consistent with the solid-state structure shown in Figure 1: the resonance at δ 100.6 ppm in the $^{13}C\{^1H\}$ NMR spectrum can be assigned to the *ipso*-carbon, and the shift to lower frequency relative to the free phosphine (δ = 138.6 ppm) suggests that the Pd−C_{ipso} interaction is retained in solution. At room temperature, however, the ^{13}C NMR spectrum shows only a single resonance (δ 127.1 ppm) for the *ortho*-carbon atoms, suggesting either that the vibration of the phenyl ring about the P−Ph bond is rapid on the NMR time scale or that an η^1-coordination mode is present in solution.

Bridging coordination of aryl phosphines is rare but not unprecedented. In fact, two examples of palladium complexes with this type of P−Ph bridging motif have been reported previously, both of which are dicationic palladium(I) dimers: the $[(dppp)Pd]_2(CF_3SO_3)_2$ species reported by van Leeuwen[14] and $[(PPh_3)Pd(MeCN)]_2(PF_6)_2$, reported by Kurosawa[15] (see Scheme 3). In both of these compounds, the Pd−C_{ipso} distances (2.385(16) and 2.336(4) Å, respectively) are shorter than the corresponding distances in complex **8**, while the Pd−C_{ortho}

Scheme 3. Previously Reported Dimers by Kurosawa[15] (a) and van Leeuwen[14] (b)

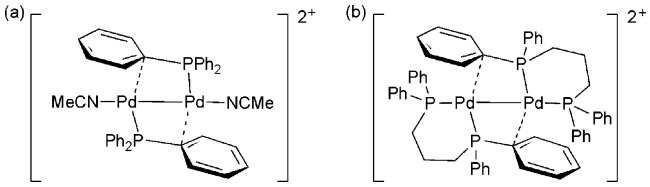

distances are rather longer (2.703(4)/2.974(4) Å and 2.89/3.01 Å, respectively), indicating a slippage toward η^1- rather than η^2-coordination of the arene ring. van Leeuwen has discussed the nature of the bonding in the $[(dppp)Pd]_2^{2+}$ cation (Scheme 3) using a highly simplified model where the dppp ligand was replaced by two PH_3 groups.[14] Despite the complete absence of a C=C double bond in their model, the Hartree−Fock-optimized geometries still reproduced the tilting of the Pd−P bonds toward the neighboring Pd atoms, with Pd···P separations of ca. 3.0 Å. As a result, the authors concluded that direct Pd···P interactions were the major factor in stabilizing the bridging coordination mode of the phosphine. The Pd···P separations of 2.92 Å in **8** are not dissimilar to those in the $[(dppp)Pd]_2^{2+}$ cation, suggesting that Pd···P interactions may also be important in this case, but the rather short and highly symmetric Pd−C_{ipso} and Pd−C_{ortho} bonds noted above indicate that interactions with the π-electron density of the arene ring cannot be ignored.

In an attempt to resolve the nature of the bonding in this system, we have conducted a series of calculations using density functional theory. The optimized structure of **8**, including the phenyl and ^{t}Bu groups on the phosphorus center, is summarized in Figure 2a. The principal features of the X-ray structure are well reproduced, in particular the Pd−Pd (2.61 Å), Pd−Br (2.56 Å), and Pd−P (2.28 Å) bond lengths. The geometry about the palladium center is also in good agreement with experiment, with optimized Pd−C_{ipso} and Pd−C_{ortho} bond lengths of 2.49 Å and a Pd···P separation of 2.99 Å. A topological analysis of the computed electron density using the atoms in molecules (AIM)[16] approach reveals the presence of bond critical points along both the Pd−C_{ipso} and Pd−C_{ortho} vectors and the corresponding bond paths exhibit a pronounced inward curvature in the proximity of the carbon atoms, a situation that is typical of an η^2-coordination mode.[17] Thus the molecular structure and the electron density indicate that the bridge is stabilized in this case by an interaction between the π-electron density on the arene ring and the remote palladium.

In our previous study on complexes of the analogous biphenyl phosphines,[12] we highlighted the importance of the steric bulk of the ^{t}Bu groups in determining the strength of the interaction between the metal center and the arene group. In order to explore this question in the context of **8**, we have reoptimized the structure of two simplified model complexes, one where the ^{t}Bu groups on the phosphine have been replaced with methyl groups (Figure 2b) and the other where they are replaced with hydrogen atoms (Figure 2c). In the case of PMe_2Ph, the tilt of the arene ring is less pronounced, and as a result, the Pd−C_{ortho} distance (2.54 Å) is now considerably longer than Pd−C_{ipso} (2.42 Å). These trends are even more exaggerated when the methyl groups are replaced with hydrogen: the P−C bond is now

(14) Budzelaar, P. H. M.; Van Leeuwen, P. W. N. M.; Roobeek, C. F.; Orpen, A. G. *Organometallics* **1992**, *11*, 23.

(15) Murahashi, T.; Otani, T.; Okuno, T.; Kurosawa, H. *Angew. Chem., Int. Ed.* **2000**, *39*, 537.

(16) Bader, R. F. W. In *Handbook of Molecular Physics and Quantum Chemisty*; Wilson, S., Vol. Ed.; John Wiley & Sons Ltd.: Chichester, U.K., 2003; Vol. 2, p 770.

(17) Macchi, P.; Proserpio, D. M.; Sironi, A. *J. Am. Chem. Soc.* **1998**, *120*, 1447.

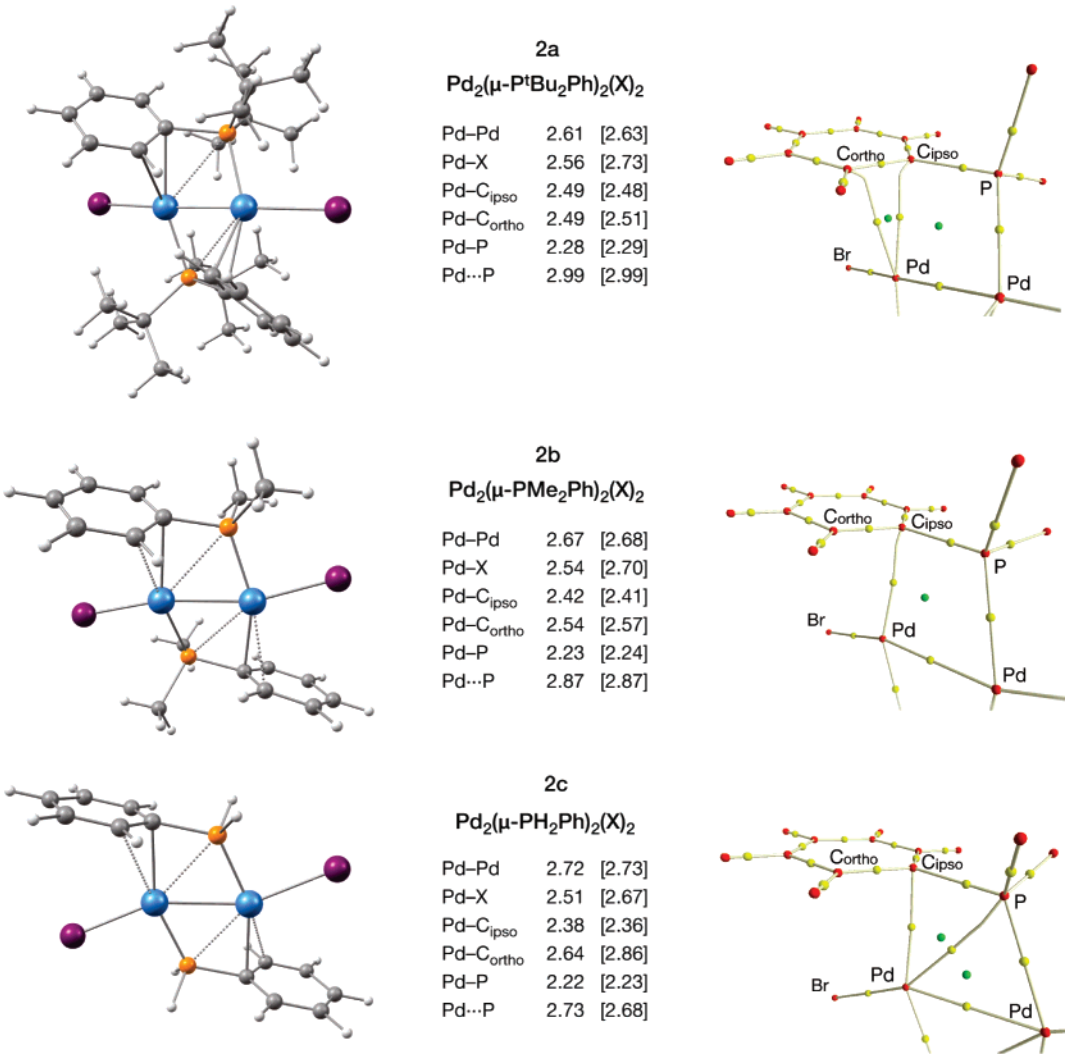

Figure 2. Optimized structures (bond lengths in Å) and partial molecular graphs of μ-PR_2Ph isomers of $Pd_2X_2(PR_2Ph)_2$ (X = Br, I) for R = ^{t}Bu, Me, H. Values in brackets are for the iodide species. In the molecular graphs red spheres indicate nuclei, yellow corresponds to (3,−1) bond critical points, and green represents (3,+1) ring critical points.

almost parallel to the Pd−Pd axis and the arene ring is perpendicular to the plane defined by the Pd−Pd−P bonds. As a result, the distinction between the Pd−C_{ortho} and Pd−C_{ipso} distances (2.64 and 2.38 Å, respectively) is even greater. The structural changes associated with the removal of the ^{t}Bu groups are accompanied by substantial changes in the topology of the electron density: the Pd−C_{ortho} bond critical point present in **8** disappears in the PMe_2Ph complex, while a new one emerges between Pd and the remote phosphorus atom in the PH_2Ph analogue. Importantly, the charge density at the new Pd−P and the Pd−C_{ipso} critical points in the latter is identical ($\rho = 0.05$), suggesting that these two interactions are of similar magnitude. Thus the bonding model that emerges from the analysis of the electron density in the PH_2Ph model system is rather different from the complete molecule **8**: in the former, the interaction between the phosphine ligand and the remote palladium is dominated by a P−C agostic bond, quite distinct from the Pd−(C═C) interaction in the latter. The methylated complex (PMe_2Ph) lies between these two extremes, with only a single critical point from the palladium to the *ipso*-carbon. While the precise correspondence between AIM critical points and chemical bonds continues to be debated,[18−20] our analysis of the electron density distributions in these three closely related systems clearly indicates that the interaction between the phosphine group and the remote palladium in any given system may contain contributions from a classic η^2-C═C bond and also from an agostic P−C interaction. Perturbations to the system due, for example, to steric effects can therefore be interpreted in terms of distortions along a continuum linking the η^2-C═C and P−C agostic limits. In the present case, the bulky ^{t}Bu groups influence the structure in a number of ways. First, and most obviously, repulsions with the bromide ligands increase the P−Pd−Br angle from 90° to 104°, imposing an almost collinear Br−Pd−Pd−Br geometry, quite distinct from the very bent structure in the model system **2c** (Pd−Pd−Br = 157°).[21] More subtly, the bulky groups increase the R−P−R angle from 101° (R = H, **2c**) to 113° (R = ^{t}Bu, **2a**), as a result of which the

(18) Poater, J.; Sola, M.; Bickelhaupt, F. M. *Chem. Eur. J.* **2006**, *12*, 2902.

(19) Maseras, F.; Lledos, A.; Costas, M.; Poblet, J. M. *Organometallics* **1996**, *15*, 2947.

(20) Bader, R. F. W. *Chem. Eur. J.* **2006**, *12*, 2896.

(21) Interestingly, a similar bending of the Pd−Pd−L angle is observed in both $[(dppp)Pd]_2^{2+}$ (161°)[14] and, to a lesser extent, $[(PPh_3)Pd(MeCN)]_2^{2+}$ (172°),[15] where the substituents on the phosphine are much less bulky. Our AIM analysis of the full $[(dppp)Pd]_2^{2+}$ system computed at the same level of theory reveals that the electron density is very similar to that in the simplified model system, with critical points between Pd and the semibridging P, as suggested by van Leeuwen, but also between the Pd center and the *ipso*-carbon, indicating a P−C agostic structure.

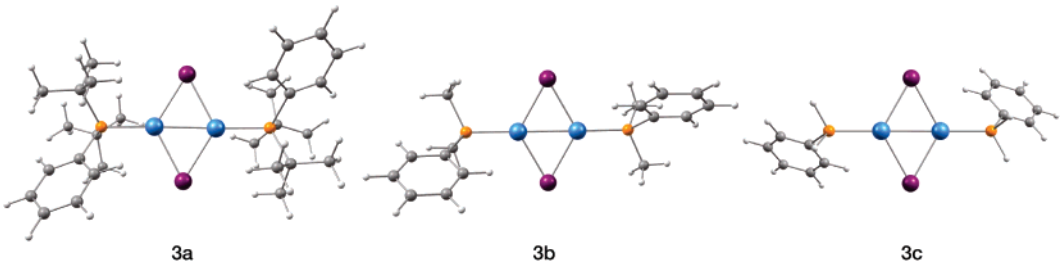

3a		3b		3c	
$Pd_2(\mu\text{-}X)_2(P^tBu_2Ph)_2$		$Pd_2(\mu\text{-}X)_2(PMe_2Ph)_2$		$Pd_2(\mu\text{-}X)_2(PH_2Ph)_2$	
E_{rel}	+2.1 [−4.4]	E_{rel}	+10.1 [+3.2]	E_{rel}	+4.0 [−1.7]
Pd–Pd	2.61 [2.67]	Pd–Pd	2.60 [2.65]	Pd–Pd	2.58 [2.63]
Pd–X	2.55 [2.68]	Pd–X	2.54 [2.67]	Pd–X	2.54 [2.67]
Pd–P	2.32 [2.33]	Pd–P	2.29 [2.29]	Pd–P	2.28 [2.29]

Figure 3. Optimized structures (bond lengths in Å) of μ-X isomers of $Pd_2X_2(PR_2Ph)_2$ (X = Br, I) for R = ^{t}Bu, Me, H, and relative energies (kcal mol^{-1}) with respect to the μ-PR_2Ph isomers of Figure 2. Values in brackets are for the iodide species.

C_{ipso}−P−Pd angle contracts from 125° to 106° (the well-known Thorpe-Ingold effect). Finally, the ^{t}Bu groups prevent the arene substituent from adopting its electronically preferred conformation where it lies perpendicular to the Pd−Pd−P bonds (as in the model system **2c**), instead forcing it to tilt toward a less crowded conformation where the plane of the ring bisects the ^{t}Bu−P−^{t}Bu angle. All three of these factors contribute toward a decrease in the separation between the remote palladium center and one of the two *ortho*-carbon atoms and, hence, drive the system toward the η^2-(C═C) limit of the continuum.

Synthesis of $Pd_2(\mu\text{-}I)_2(P^tBu_2Ph)_2$ (9). Once the unexpected semibridging coordination mode of the phosphine in **8** had been established, we were interested to know whether the same structural features would be present in the iodide analogue. However, since the Pd(COD)I_2 starting material is not readily available and moreover is difficult to purify, a different synthetic approach was required. We have previously established that palladium(I)−halide dimers can be prepared by the reaction between a palladium(0) compound and the corresponding halide source (see Scheme 1).[7] On the basis of this approach, 0.5 equiv of CHI_3 (previously shown to be a good source of iodide in the synthesis of palladium dimers) was added to $Pd(P^tBu_2Ph)_2$ (generated in situ from $Pd_2(dba)_3$ and 2 equiv of P^tBu_2Ph), yielding a dark brown solution. The solvent was then removed under reduced pressure and the residue washed with cold diethyl ether and recrystallized from THF at low temperature to yield $Pd_2(\mu\text{-}I)_2(P^tBu_2Ph)_2$ (**9**) as a purple solid. Repeated attempts to obtain single crystals suitable for X-ray crystallography have proved unsuccessful, but the formulation of **9** was confirmed by elemental analysis and MALDI(+) mass spectrometry, which revels a peak at 910 amu corresponding to the molecular ion $[M]^+$. Despite the lack of crystallographic data, we can infer from the NMR characteristics of **9** that its structure is quite different from that of **8**. The $^{31}P\{^1H\}$ NMR spectrum of this complex showed a singlet at 81.7 ppm, quite similar to the value in **8**, but the $^{13}C\{^1H\}$ NMR spectra of the two species are quite distinct. In particular, the resonance for the *ipso*-carbon of P^tBu_2Ph appears at δ 134.4 ppm in **9**, a very similar value to that of the free phosphine and very different from the δ 100.6 ppm resonance characteristic of the semibridging phosphine architecture in **8**. On the basis of this data, we therefore propose that the iodide complex, **9**, features the same μ-iodo architecture seen in its P^tBu_3 analogue, $Pd_2(\mu\text{-}I)_2(P^tBu_3)_2$, rather than the semibridging phosphine structure found in **8**.

To understand the adoption of different bonding modes of the phosphine and halides in **8** and **9**, we have conducted a more detailed survey of the potential energy surface for both complexes. This study reveals minima corresponding to the halide-bridged isomers (Figure 3) in addition to the semibridged phosphine species discussed previously (Figure 2). The geometry of the $Pd_2(\mu\text{-}I)_2$ core shown in Figure 3a is very similar to that in the known structure of $Pd_2(\mu\text{-}I)_2(P^tBu_3)_2$, with optimized Pd−Pd and Pd−I separations of 2.61 and 2.54 Å, respectively. In the context of the current discussion, the critical feature is that while the μ-halide structure is marginally less stable than its semibridged phosphine counterpart for the bromide complex (ΔE = 2.1 kcal mol^{-1}), the opposite is true for the iodide analogue (ΔE = −4.4 kcal mol^{-1}), consistent with experiment. We have noted previously that the precise nature of the bonding within the semibridging architecture is highly sensitive to steric factors, but the μ-halide structure seems relatively robust, and the geometries are not strongly influenced by the removal of the ^{t}Bu groups (compare Figures 3a, 3b, and 3c). Given the very small energy differences between the two isomeric forms in each case, it may be that subtle differences in the steric interactions between the phosphine and the halide cause the switch in structure.

Conclusions

The results presented here, together with our previous investigations into the formation of palladium dimers with ^{t}Bu and biphenyl phosphines, demonstrate the important role of both the steric and electronic properties of the phosphine in determining the final structure of the dinuclear compounds. While the bulky and electron-rich phosphine P^tBu_3 yields the $Pd_2(\mu\text{-}X)_2(P^tBu_3)_2$ dimers (with terminal P^tBu_3 and bridging halides), the biphenyl phosphines P^tBu_2(Bph-R) yield the $[Pd_2X(\mu\text{-}X)\{\mu\text{-}P^tBu_2(Bph\text{-}R)\}]$ species, where the metal centers are bridged by both the terminal arene ring of the biphenyl moiety and one halide. The molecular structure of $Pd_2Br_2(\mu\text{-}P^tBu_2Ph)_2$ (**8**) shows a coordination geometry that is dramatically different from either of these: each phosphine is directly coordinated to one of the palladium centers via the phosphorus atom but also to the second palladium via the phenyl substituent on the phosphine. Density functional theory reveals that the interaction between the bridging phosphine and the remote palladium center contains contributions from both the C═C π and P−C σ bonds. Subtle changes in the steric demand of the phosphine can alter the relative contributions of these two components of the bond and, hence, can cause significant changes in structure.

Experimental Details

General Comments. All experimental procedures were carried out using standard high-vacuum and Schlenk line techniques under

an atmosphere of dry argon. Glassware was dried in an oven at 150 °C prior to use. CH_2Cl_2, hexane, THF, methanol, diethyl ether, and toluene were dried using a solvent purification system (SPS, Innovative-Technology) and degassed with argon prior to use. ^1H, ^{13}C, and ^{31}P NMR spectra were recorded on a Bruker Avance 400 or Bruker Avance 500 spectrometer and referenced to residual ^1H and ^{13}C signals of the solvents or 85% H_3PO_4 as an external standard (^{31}P). The compounds Pd(COD)Br_2, $[Pd_2(dba)_3]\cdot C_6H_6$, and P^tBu_2Ph were synthesized following literature procedures.[22−24]

Synthesis of $Pd_2Br_2(P^tBu_2Ph)_2$ (8). $Pd_2(dba)_3\cdot C_6H_6$ (209 mg, 0.210 mmol) was dissolved in toluene (20 mL), and a solution of P^tBu_2Ph (1.04 mL of a 0.773 M toluene solution, 0.840 mmol) in toluene was added with stirring. After 2 h, Pd(COD)Br_2 (105 mg, 0.281 mmol) was added and the reaction mixture stirred overnight to yield a dark brown precipitate. After filtration the precipitate was washed with diethyl ether (2 × 10 mL). Recrystallization from CH_2Cl_2/hexane yielded a brown solid. Yield: 112 mg, (49%). Single crystals suitable for X-ray crystallographic studies were grown from a chloroform solution. ^1H NMR (CD_2Cl_2, 500 MHz): δ 8.30 (dd, J_{HH} = 8.3 Hz, J_{HP} = 8.3 Hz, 4H, *o*-Aryl-H), 7.87 (t, $^2J_{HH}$ = 7.4 Hz, 2H, *p*-Aryl-H), 7.68 (dd, J_{HH} = 7.4 Hz, 4H, *m*-Aryl-H), 1.48 (d, $^3J_{PH}$ = 14.8 Hz, 36H, C(CH_3)$_3$). $^{13}C\{^1H\}$ NMR (126 MHz, CD_2Cl_2): δ 136.3 (*p*-Aryl-C), 132.2 (d, J_{PC} = 8.6 Hz, *m*-Aryl-C), 127.1 (*o*-Aryl-C), 100.6 (*ipso*-Aryl-C), 38.8 (d, J_{PC} = 14.7 Hz, $C(CH_3)_3$), 31.2 (C(CH_3)$_3$). $^{31}P\{^1H\}$ NMR (202 MHz, CD_2Cl_2): δ 76.9 (s). FAB-MS: m/z^+ 818 $[M]^+$, 737 $[M - Br]^+$. Anal. Calcd for $C_{28}H_{46}Br_2P_2Pd$: C, 41.15; H, 5.67. Found: C, 41.05; H, 5.60.

Synthesis of $Pd_2I_2(P^tBu_2Ph)_2$ (9). To a solution of $Pd_2(dba)_3\cdot C_6H_6$ (102 mg, 0.102 mmol) in toluene (10 mL) was added P^tBu_2Ph (265 μL of a 0.773 M toluene solution) in toluene. After 2 h CHI_3 (20 mg, 0.051 mmol) was added as a solid. The reaction solution was stirred for an additional hour, after which time the solvent was removed under reduced pressure. The crude product was recrystallized from THF at −4 °C to obtain a dark purple solid, which was washed twice with cold diethyl ether and dried under vacuum. Yield: 25 mg (21%). ^1H NMR (400 MHz, THF-d_8): δ 8.11−8.02 (m, 4H), 7.45−7.32 (m, 6H), 1.25 (t, $^3J_{PH}$ = 7.00 Hz, 36H, C(CH_3)$_3$). $^{13}C\{^1H\}$ NMR (126 MHz, THF-d_8): δ 137.8 (*C*-arom.), 134.4 (d, J_{PC} = 11.9 Hz, *ipso*-C-Aryl), 131.1 (d, J_{PC} = 10.1 Hz, *C*-arom.), 128.1 (d, J_{PC} = 4.69 Hz, C-arom.), 34.2 (d, J_{PC} = 5.55 Hz, $C(CH_3)_3$), 34.1 (d, J_{PC} = 5.55 Hz, $C(CH_3)_3$), 30.9 (d, J_{PC} = 4.69 Hz; C(CH_3)$_3$), 30.8 (d, J_{PC} = 4.16 Hz, C(CH_3)$_3$). $^{31}P\{^1H\}$ NMR (162 MHz, C_6D_6): δ 81.7 (s). MALDI-MS: m/z^+ 910 $[M]^+$. Anal. Calcd for $C_{28}H_{46}I_2P_2Pd$: C, 36.90; H, 5.09. Found: C, 36.91; H, 5.40.

X-ray Crystallography. Crystals of **8** (as a chloroform monosolvate) were obtained by crystallization in a saturated chloroform solution at room temperature. The measured crystal was prepared under inert conditions immersed in perfluoropolyether as protecting oil for manipulation. *Data collection*: Measurements were made on a Bruker-Nonius diffractometer equipped with a APPEX 2 4K CCD area detector, a FR591 rotating anode with Mo Kα radiation, Montel mirrors as monochromator, and a Kryoflex low-temperature device (T = −173 °C). Full-sphere data collection was used with ω and φ scans. *Programs used*: Data collection, Apex2 V. 1.0−22 (Bruker-Nonius 2004); data reduction, Saint+ Version 6.22 (Bruker-Nonius 2001); and absorption correction, SADABS V. 2.10 (2003). *Structure solution and refinement*: SHELXTL Version 6.10 (Sheldrick, 2000) was used. *Crystal data for* ***8***$\cdot CHCl_3$: $C_{29}H_{47}Br_2Cl_3P_2Pd_2$, M = 936.58, monoclinic, space group $P2_1/c$, a = 11.368(2) Å, b = 28.186(5) Å, c = 11.873(2) Å, β = 112.828(4)°, V = 3506.6(11) Å^3, Z = 4, μ = 3.643 mm^{-1}, density = 1.774 Mg/m^3, R1 = 0.0411($I > 2\sigma(I)$)/0.0850(all data) and wR2 = 0.0810($I > 2\sigma(I)$)/ 0.0921(all data), 10 601 reflections with $I > 2\sigma(I)$, 16 064 independent reflections (R_{int} = 0.0693) with a total measured 54 952 reflections, goodness-of-fit on F^2 = 1.009, largest diff peak (hole) = 1.126 (−1.444) e Å^{-3}.

Computational Details. Full unconstrained geometry optimizations were carried out with the one-parameter hybrid mPW1PW91 density functional,[25] which has been shown to handle reliably the weak interactions in palladium−arene systems. All reported structures were verified as true minima. Pd, Br, and I were described with the Hay−Wadt effective core potentials along with the corresponding valence basis sets (LANL2DZ).[26−28] Extra sets of d polarization functions were added to the halides (α_d = 0.428 for Br, α_d = 0.289 for I).[29] We note that the accuracy of relative energies obtained with the LANL2DZ basis has been questioned for correlated HF-based methods,[30] but the inclusion of higher angular momentum functions does not appear to be critical in DFT calculations.[31,32] The 6-31G(d) basis sets were employed for phosphorus and the atoms of the phenyl group, whereas the STO-3G basis sets were used for the atoms of the ^{t}Bu groups. All calculations were performed with the Gaussian03 series of programs.[33] Wavefunction files for the AIM analysis were obtained by single-point calculations using the all-electron DGDZVP basis sets for Pd, Br, and I.[34] Subsequent analysis of the electron densities and construction of molecular graphs were carried out with the AIM2000 program.[35]

The supplementary crystallographic data for this paper (CCDC 613416) can be obtained free of charge via www.ccdc.cam.ac.uk/conts/retrieving.html (or from the Cambridge Crystallographic Data Centre, 12 Union Road, Cambridge CB2 1EZ, U.K.; fax: +44 1223 336033 or e-mail: deposit@ccdc.cam.ac.uk).

Acknowledgment. We thank EPSRC (U.K.) (GR/R74970/01 and GR/R74963/01), the ICIQ Foundation (Spain), and ICREA (Spain) for financial support and Johnson Matthey for a loan of $PdCl_2$. Dr. Gabriel Gonzalez and Mr. Kerman Gómez are thanked for their help with the NMR data. D.A.P.'s visit to ICIQ and his calculations in CESCA/CEPBA were funded by the HPC-EUROPA project (RII3-CT-2003-506079), with the support of the European Community−Research Infrastructure Action under the FP6 "Structuring the European Research Area" Programme.

Supporting Information Available: Cartesian coordinates and absolute energies for all computed structures. Complete reference for Gaussian03. Crystallographic data (CIF). This material is available free of charge via the Internet at http://pubs.acs.org.

OM060712J

(22) Drew, D.; Doyle, J. R. *Inorg. Synth.* **1990**, *28*, 346.
(23) Ukai, T.; Kawazura, H.; Ishii, Y.; Bonnet, J. J.; Ibers, J. A. *J. Organomet. Chem.* **1974**, *65*, 253.
(24) Trippett, S.; Corfield, J. R.; De'ath, N. J. **1971**, 1930.
(25) Adamo, C.; Barone, V. *J. Chem. Phys.* **1998**, *108*, 664.
(26) Hay, P. J.; Wadt, W. R. *J. Chem. Phys.* **1985**, *82*, 270.
(27) Hay, P. J.; Wadt, W. R. *J. Chem. Phys.* **1985**, *82*, 299.
(28) Wadt, W. R.; Hay, P. J. *J. Chem. Phys.* **1985**, *82*, 284.
(29) Hoellwarth, A.; Boehme, M.; Dapprich, S.; Ehlers, A. W.; Gobbi, A.; Jonas, V.; Koehler, K. F.; Stegmann, R.; Veldkamp, A.; et al. *Chem. Phys. Lett.* **1993**, *208*, 237.
(30) de Jong, G. T.; Sola, M.; Visscher, L.; Bickelhaupt, F. M. *J. Chem. Phys.* **2004**, *121*, 9982.
(31) de Jong, G. T.; Geerke, D. P.; Diefenbach, A.; Bickelhaupt, F. M. *Chem. Phys.* **2005**, *313*, 261.
(32) de Jong, G. T.; Bickelhaupt, F. M. *J. Chem. Theor. Comput.* **2006**, *2*, 322.
(33) Frisch, M. J.; et al. *Gaussian 03*, Revision c.02; Gaussian Inc.: Wallingford, CT, 2004.
(34) Godbout, N.; Salahub, D. R.; Andzelm, J.; Wimmer, E. *Can. J. Chem.* **1992**, *70*, 560.
(35) Biegler-König, F.; Schönbohm, J. *AIM2000*, version 2.0; Büro für Innovative Software, 2002.